Two-photon fluorescence imaging of intracellular hydrogen peroxide with chemoselective fluorescent probes

Journal of Biomedical Optics

SPIEDigitalLibrary.org/jbo

Two-photon fluorescence imaging of intracellular hydrogen peroxide with chemoselective fluorescent probes

Hengchang Guo
Hossein Aleyasin
Scott S. Howard
Bryan C. Dickinson
Vivian S. Lin
Renee E. Haskew-Layton
Chris Xu
Yu Chen
Rajiv R. Ratan

SPIE

Two-photon fluorescence imaging of intracellular hydrogen peroxide with chemoselective fluorescent probes

Hengchang Guo,[a,b] Hossein Aleyasin,[b] Scott S. Howard,[c,d] Bryan C. Dickinson,[e] Vivian S. Lin,[f] Renee E. Haskew-Layton,[b] Chris Xu,[c] Yu Chen,[a] and Rajiv R. Ratan[b]
[a]University of Maryland, Fischell Department of Bioengineering, College Park, Maryland 20742
[b]Weill Medical College of Cornell University, Burke Medical Research Institute, White Plains, New York 10605
[c]Cornell University, School of Applied and Engineering Physics, Ithaca, New York 14853
[d]University of Notre Dame, Department of Electrical Engineering, Notre Dame, Indiana 46556
[e]Harvard University, Department of Chemistry and Chemical Biology, Cambridge, Massachusetts 02138
[f]University of California, Department of Chemistry, Berkeley, California 94720

Abstract. We present the application of two-photon fluorescence (TPF) imaging to monitor intracellular hydrogen peroxide (H_2O_2) production in brain cells. For selective imaging of H_2O_2 over other reactive oxygen species, we employed small-molecule fluorescent probes that utilize a chemoselective boronate deprotection mechanism. Peroxyfluor-6 acetoxymethyl ester detects global cellular H_2O_2 and mitochondria peroxy yellow 1 detects mitochondrial H_2O_2. Two-photon absorption cross sections for these H_2O_2 probes are measured with a mode-locked Ti:sapphire laser in the wavelength range of 720 to 1040 nm. TPF imaging is demonstrated in the HT22 cell line to monitor both cytoplasmic H_2O_2 and localized H_2O_2 production in mitochondria. Endogenous cytoplasmic H_2O_2 production is detected with TPF imaging in rat astrocytes modified with D-amino acid oxidase. The TPF H_2O_2 imaging demonstrated that these chemoselective probes are powerful tools for the detection of intracellular H_2O_2. [DOI: 10.1117/1.JBO.18.10.106002]

Keywords: two-photon fluorescence imaging; hydrogen peroxide; reactive oxygen species; fluorescent probe; oxidative stress; molecular imaging.

Paper 130259R received Apr. 17, 2013; revised manuscript received Aug. 16, 2013; accepted for publication Aug. 28, 2013; published online Oct. 1, 2013.

1 Introduction

Hydrogen peroxide (H_2O_2), a common reactive oxygen species (ROS) found in biological systems, is now recognized as an intracellular second messenger for cellular signaling that exerts diverse physiological and pathological effects.[1–7] The aberrant production or accumulation of H_2O_2 within cellular mitochondria over time due to oxidative stress or genetic mutation is connected to serious pathological conditions including cancer,[8] diabetes,[9] and neurodegenerative diseases such as Alzheimer's, Parkinson's, and Huntington's diseases, as well as stroke.[10–12] In addition, H_2O_2 is involved in therapeutic processes such as wound healing, stem cell proliferation, and an adaptive response in astrocytes leading to neuronal protection.[1,2,7,13]

A substantial challenge in elucidating the diverse roles of H_2O_2 in complex biological environments is the lack of methods to determine the spatial and temporal dynamics of this reactive oxygen metabolite in living systems. For the detection of ROS production *in vitro*, several fluorescent probes have been developed based on small molecules, fluorescent proteins, and nanoparticles.[3,14–19] Among these technologies, small molecule probes offer an attractive approach to ROS detection due to their general compatibility with an array of biological systems without external activating enzymes and genetic manipulation. However, traditional small molecule probes such as dichlorofluorescein (DCF) derivatives detect multiple types of reactive small molecules, including other ROS such as superoxide radical ($O_2^{\bullet}$), hydroperoxy radical ($HO_2^{\bullet}$), singlet oxygen ($^1O_2$), peroxy radical ($RO_2^{\bullet}$), and reactive nitrogen species;[16] they are not specific for H_2O_2. In addition, DCF derivatives cannot be targeted to specific intracellular compartments.[14] To overcome the disadvantages of existing methods for detecting ROS, new chemoselective fluorescent indicators featuring a boronate-based molecular detection mechanism have been developed,[3] which provide improved selectivity for H_2O_2 over related ROS, particularly superoxide, nitric oxide, and hydroxyl radical. These probes include peroxyfluor-2 (PF2), peroxy yellow 1 (PY1), peroxy orange 1 (PO1), peroxyfluor-6 acetoxymethyl ester (PF6-AM), mitochondria peroxy yellow 1 (MitoPY1), etc.[2,3,18,20–22]

However, conventional confocal microscopy has limitations for use in real time *in vivo* H_2O_2 imaging, including photodamage, photobleaching, and limited imaging depth. Furthermore, prolonged visible light exposure can result in artifactual ROS generation and signal amplification.[23,24] Therefore, two-photon imaging of H_2O_2 offers an attractive alternative to overcome many of these limitations.[25–27] We report two-photon fluorescence (TPF) imaging for the detection of intracellular cytoplasmic

Address all correspondence to: Chris Xu, Cornell University, School of Applied and Engineering Physics, 276 Clark Hall, Ithaca, New York 14853. Tel: +1-607-255-1460; E-mail: chris.xu@cornell.edu; or Yu Chen, University of Maryland, Fischell Department of Bioengineering, 2218 Jeong H. Kim Engineering Building, College Park, Maryland 20742. Tel: +1-301-405-3439; Fax: +1-240-554-1688; E-mail: yuchen@umd.edu; or Rajiv R. Ratan, Burke Medical Research Institute, 785 Mamaroneck Avenue, White Plains, New York 10605. Tel: +1-914-597-2851; Fax: +1-914-597-2225; E-mail: rrr2001@med.cornell.edu

and mitochondrial H_2O_2 production in live cells using a variety of next-generation boronate-based probes such as PF6-AM and MitoPY1. Two-photon absorption (TPA) cross sections of these probes were measured with a Ti:sapphire laser by comparison with the TPA cross section of fluorescein.[26,28] To our knowledge, this is the first two-photon characterization of these particular chemoselective probes and provides a clear example for the detection of intracellular H_2O_2 production with TPF imaging.

2 Materials and Methods

2.1 *Chemoselective Fluorescent Probes*

We characterized a series of previously reported chemoselective probes with three useful colors: green (PF2 and PF6-AM), yellow (PY1 and MitoPY1), and orange (PO1). Figure 1 illustrates reaction of H_2O_2 with these probes, which are based on fluorescein/rhodamine derivatives. The aryl boronate to phenol chemical switch is utilized for selective detection of H_2O_2 over other ROS. Upon reaction with H_2O_2, a highly fluorescent product is released and can be assayed by fluorescence imaging. To improve the cell membrane permeability and trap the probe in the cytosol, PF6-AM was modified from PF6 with acetoxymethyl ester groups.[2,26] Upon penetration of the cell membrane, PF6-AM is deprotected by intracellular esterases, releasing the dianionic PF6 that is then trapped in the cytosol [Fig. 1(e)]. MitoPY1 [Fig. 1(d)] was derived from PY1 to include a combination of a boronate-based switch and a mitochondrial-targeting phosphonium moiety for the detection of H_2O_2 localized to cellular mitochondria.[18]

2.2 *TPA Measurement*

A basic parameter to characterize a fluorophore for TPF imaging is the TPA cross section. TPA spectra were measured using a Ti:sapphire laser (Spectra Physics Mai Tai HP) operating at 720 to 1040 nm, 100 fs pulse width, and 80 MHz repetition rate. The scheme of experimental setup was described in Xu and Webb.[28] Before the measurement, we verified that the TPF intensity increases with the square of the excitation power.

TPF intensity is related to spatial dependence and temporal dependence such as laser parameters and system collection condition.[28] A direct measurement of TPA cross section is difficult. Therefore, absolute TPA cross section values of fluorescent probes (δ_P) were calculated by comparison with the TPF intensity of fluorescein (δ_F) in Eq. (1):[28]

$$\delta_P = \delta_F \frac{F_P}{F_F}\frac{\Phi_F}{\Phi_P}\frac{c_F}{c_P}\frac{\Phi_{F-\mathrm{PMT}}}{\Phi_{P-\mathrm{PMT}}}, \tag{1}$$

where F_P and F_F are the fluorescence intensity measured with a photon counting photomultiplier tube (PMT) at the same laser power excitation, Φ_P and Φ_F are the two-photon-excited fluorescence quantum yields of the probes assumed to be same to that of single-photon excited, c_P and c_F are the concentrations of the probes, $\Phi_{P-\mathrm{PMT}}$ and $\Phi_{F-\mathrm{PMT}}$ are the quantum efficiency of the PMT (Hamamatsu R7600U-200) obtained from the manufacturer's data. The system collection efficiency, estimated to be the same for the probes, are based on its fluorescence emission spectrum, the measured numerical aperture (NA) and transmission of the objective lens, and the transmission of the filters.[28] The fluorescent probes were measured with the same measurement conditions as fluorescein, therefore these

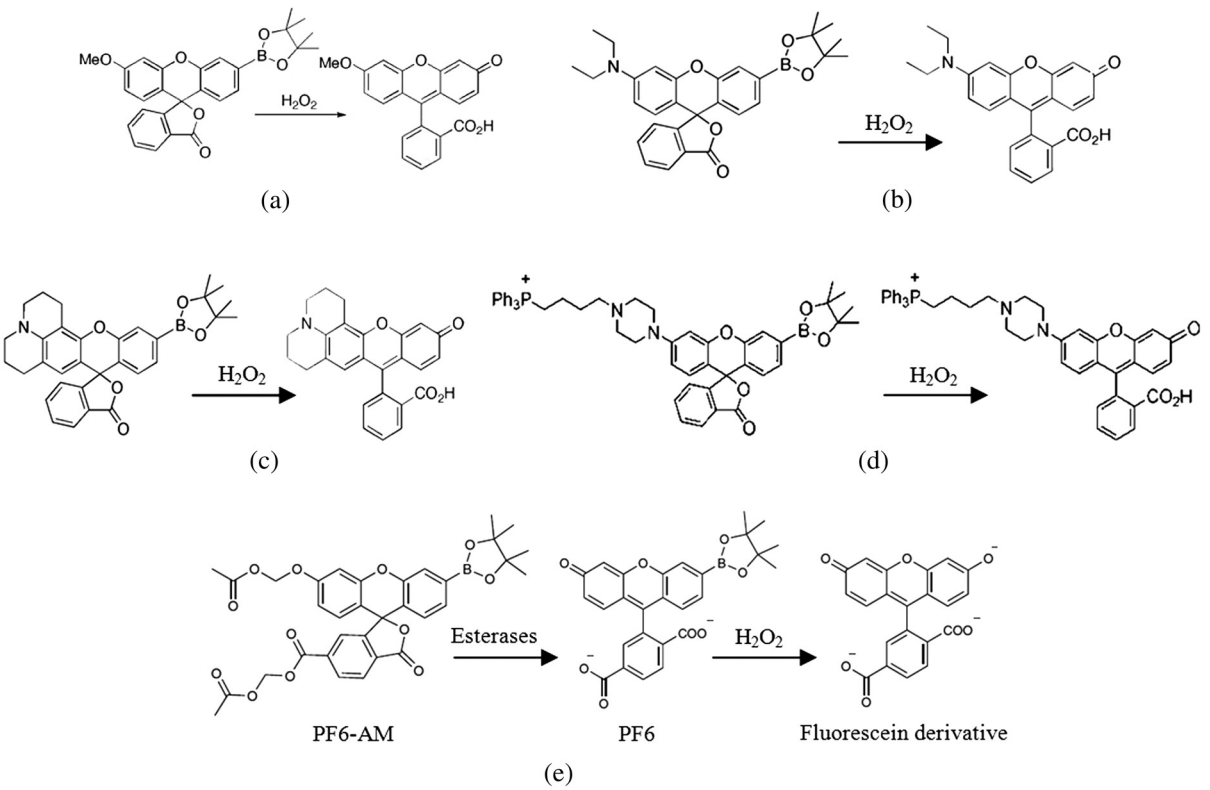

Fig. 1 Chemoselective fluorescent probes for H_2O_2 detection. (a) PF2, (b) PY1, (c) PO1, (d) MitoPY1, and (e) PF6-AM.

measurements can be used to calculate TPA cross section without explicitly characterizing pulse shape by comparing measured values to those found in Ref. 28.

PF2, PY1, PO1, MitoPY1, and DCF were diluted to form a 20 μM solution in 1× phosphate buffered saline (PBS) buffer. We then added high concentrations of H_2O_2 (100 μM) to ensure complete deprotection. PF6-AM (20 μM) in 1× PBS buffer was incubated with both H_2O_2 (100 μM) and esterase (10 U/mL) from rabbit liver (Sigma–Aldrich #040566) to deprotect the boronate and the AM-esters.

2.3 *Confocal and Two-photon Microscopy*

H_2O_2 imaging was performed with a commercial laser scanning inverted microscope system (Zeiss 710NLO) including configuration both for confocal and TPF microscopy. This system was equipped with a 488-nm argon laser and a Ti:sapphire laser (Coherent Chameleon Vision II) with 690- to 1080-nm wavelength, 140-fs pulse width, and 80-MHz repetition rate. We operated the Ti:sapphire laser at 770 nm, a wavelength for TPF imaging of PF6-AM, MitoPY1, and Hoechst 33342. A 20 × /0.80 NA objective (Zeiss Plan-Apochromat) was employed to focus the excitation laser beam onto cells and was also used for fluorescence collection into the PMTs. A prism-based 34-channel QUASAR detection unit was used for tunable spectral band-width collection without traditional band-pass filters. A 5% CO_2 circulation and 37°C thermal chamber was used for live cell imaging.

2.4 *Cell Culture*

All animal procedures were performed according to protocols approved by the Institutional Animal Care and Use Committee of the Weill Medical College of Cornell University. The HT22 cell, an immortal neuroblast line originated from hippocampal neurons, and primary rat astrocytes were cultured in 35-mm Petri dishes with a cover-glass at the bottom.

Primary astrocyte cultures were prepared from the cerebral cortices of Sprague-Dawley rat pups (P1-3) as described in Haskew-Layton et al.[1] In brief, astrocyte cultures were grown for about 2 weeks until reaching confluency in minimal essential medium (Invitrogen) supplemented with 10% horse serum and 25 U/mL penicillin plus 25 g/mL streptomycin. Once confluent, the astrocytes were treated with 8 μM cytosine-D-arabinofuranoside (Ara-C), a mitotic inhibitor for ~3 days, to kill off contaminating cells. The astrocytes were used for experiments at 2 to 3 weeks in culture.

2.5 *Intracellular H_2O_2 Production*

H_2O_2 is generally produced by the dismutation of mitochondrial superoxide or as a product of enzymatic activity. To mimic mitochondrial H_2O_2 production, HT22 cells were treated with the complex I respiratory chain inhibitor rotenone.[29]

To generate cytoplasmic H_2O_2, we used an enzymatic method for intracellular H_2O_2 production in astrocytes.[1] Primary astrocytes were transduced with adenoviruses containing the cDNA for cytoplasmic D-amino acid oxidase (DAAO) for 4 days. DAAO oxidatively deaminates D-amino acids using flavin adenin denucleotide (FAD) as an electron acceptor. At the same time, DAAO uses molecular O_2 to oxidize FAD, during which time H_2O_2 is produced as a byproduct. H_2O_2 is therefore produced in a dose-dependent manner relative to the concentration of D-alanine added. Following DAAO-transduction, astrocytes were incubated with 5 μM PF6-AM and Hoechst 33342. D-Alanine (2 mM) stimulated H_2O_2 production in DAAO astrocytes was then detected; the cells were supplemented with the DAAO cofactor FAD (2.5 μM).

3 Results and Discussions

3.1 *TPA Spectrum*

The two-photon activation times, single-photon absorption and emission peaks, and quantum yields of the probes were measured and are shown in Table 1. Activation time refers to the average time when the TPF intensity increases to $1/e$ of the saturation intensity. This activation time is related to the deprotection efficiency. Compared with the commonly used nonspecific probe DCF, the chemoselective probes demonstrated much faster responses to H_2O_2.

Figure 2 shows single-photon absorption and fluorescence emission spectra, and absolute values of TPA cross sections for the H_2O_2 probes PF2, PY1, PO1, MitoPY1, and PF6-AM. As a comparison, Fig. 2(f) shows the TPA cross section of DCF. The peak cross section values of chemoselective probes are comparable to that of fluorescein,[28] which is sufficiently large for two-photon imaging *in vitro* or *in vivo*. To ensure that H_2O_2 has deprotected the boronate, the TPF spectra were measured at least 1 h after H_2O_2 addition. Then, the TPA cross section was calculated based on the above Eq. (1) and the parameter in Table 1.

We measured several color probes here so that multicolor imaging can be performed with minimum fluorescence bleed-through with other co-staining dyes. Figure 2 helps us to select co-staining dyes for single excitation wavelength two-photon multicolor imaging.

3.2 *TPF Imaging of Intracellular H_2O_2*

Figure 3 shows intracellular TPF imaging of H_2O_2 in HT22 cells stained with PF6-AM. The cells were incubated in PF6-AM solution for 20 min and the nuclei were stained with Hoechst 33342. Figures 3(a) and 3(b) show the H_2O_2 concentration increasing in cells after the addition of exogenous H_2O_2. This result demonstrates that PF6-AM is capable of detecting cytoplasmic H_2O_2. Figures 3(c) and 3(d) demonstrate

Table 1 Optical parameters of H_2O probes.

Probes	Absorption peak (nm)	Emission peak (nm)	Quantum yields	Activation time[a] (min)
PF2	455	515	0.27	3 ± 1
PY1	520	550	0.12	3 ± 3
PO1	540	570	0.46	3 ± 3
MitoPY1	510	530	0.405	24 ± 5
PF6-AM	460	520	0.94	14 ± 1
DCF	500	525	0.9 to 0.95	48 ± 1

[a]Activation time τ is obtained from the simulation of this equation $\text{sat} - (\text{sat} - \text{int}) \times \exp(-x/\tau)$ using Qtiplot software.

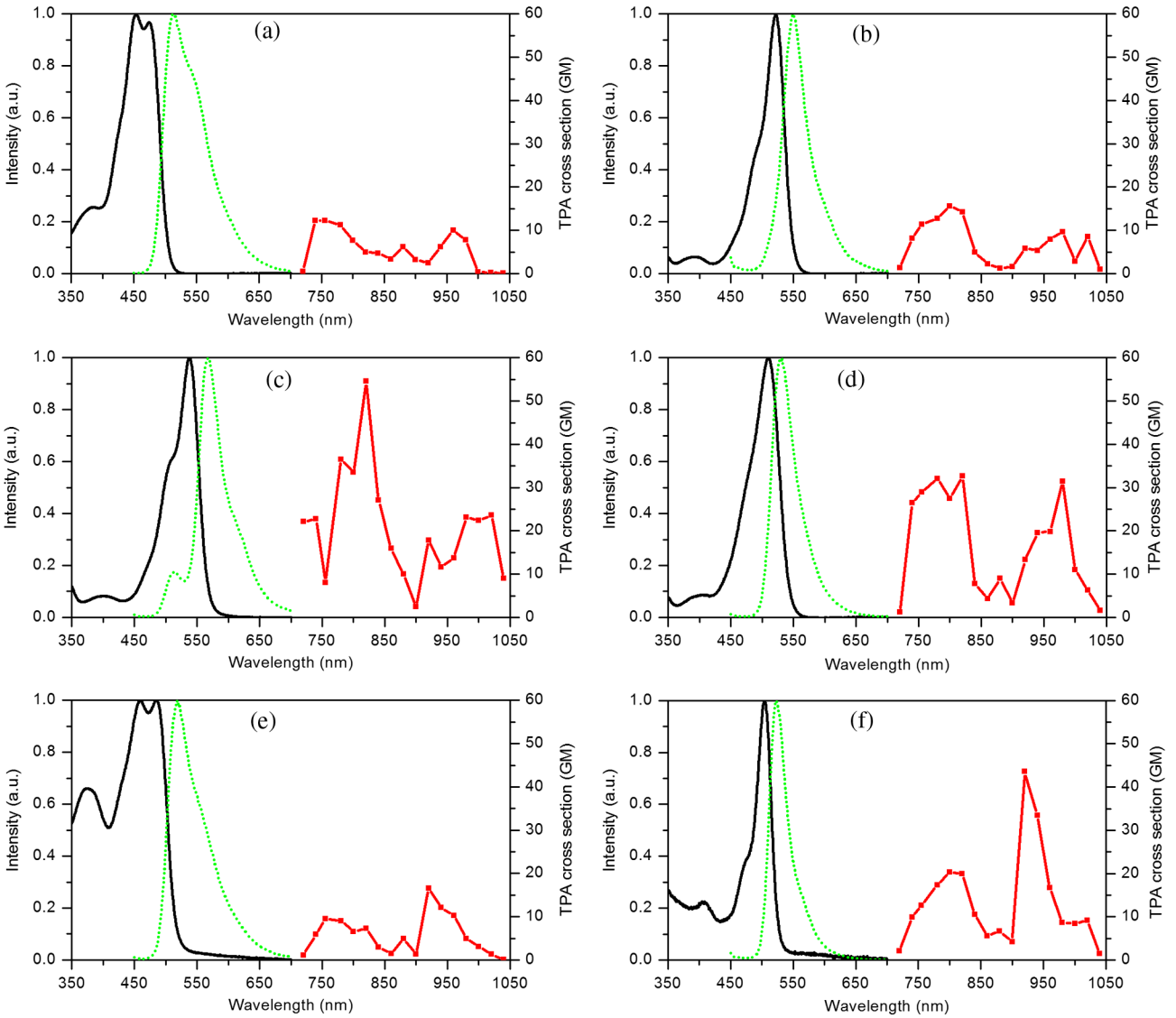

Fig. 2 Single-photon absorption spectrum (black line), fluorescence emission spectrum (green-dot line), and absolute value of two-photon absorption spectrum (red-symbol line) for H_2O_2 probes in 1× phosphate buffered saline solution. GM = 1×10^{-50} cm^4 S/photon. (a) PF2, (b) PY1, (c) PO1, (d) MitoPY1, (e) PF6-AM, and (f) DCF.

endogenous H_2O_2 production induced by rotenone, which resulted in bright punctate staining patterns that are likely the sources of H_2O_2 production.

To improve the signal-to-background ratio and target mitochondrial H_2O_2 production, we used MitoPY1 for mitochondrial labeling and detection of localized H_2O_2 production. Figure 4 shows an overlay of TPF imaging of MitoPY1 labeled mitochondrial H_2O_2 production and MitoTracker Red labeled mitochondria. Rotenone was added to the HT22 cells after they were incubated with 5 μM MitoPY1 for 25 min. Then, MitoTracker Red was added after another 60 min to ensure that MitoPY1 was targeted to the mitochondria in HT22 cells.

Figure 5 shows TPF imaging of cytoplasmic H_2O_2 production induced by DAAO in astrocytes. PF6-AM and Hoechst 33342 were co-excited with 770-nm laser pulses. The TPA cross section of FAD at 770 nm is only $\times 10^{-3}$ that of PF6AM.[30] Therefore, the fluorescence of FAD is only a weak background signal. The fluorescence intensity in Fig. 5 shows cytoplasmic H_2O_2 increasing from the time (a) 1 min, (b) 6 min, and (c) 25 min after the addition of D-alanine and FAD.

3.3 *Discussion*

The involvement of H_2O_2 in cellular signaling related to cancer and neurodegenerative diseases has motivated the development of imaging technologies for measuring intracellular H_2O_2 concentration and dynamics in cellular compartments. Previous studies have relied on a horseradish peroxidase/Amplex Red substrate system to measure extracellular H_2O_2 production using a spectrophotometer (Spectramax Plus 384; Molecular Devices).[1] However, DAAO derived H_2O_2 production provides a controllable scale ideal for intracellular H_2O_2 measurements. TPF signal intensity is linearly related to the fluorophore concentration. Therefore, TPF imaging provides the possibility for quantification of localized intracellular H_2O_2 production.

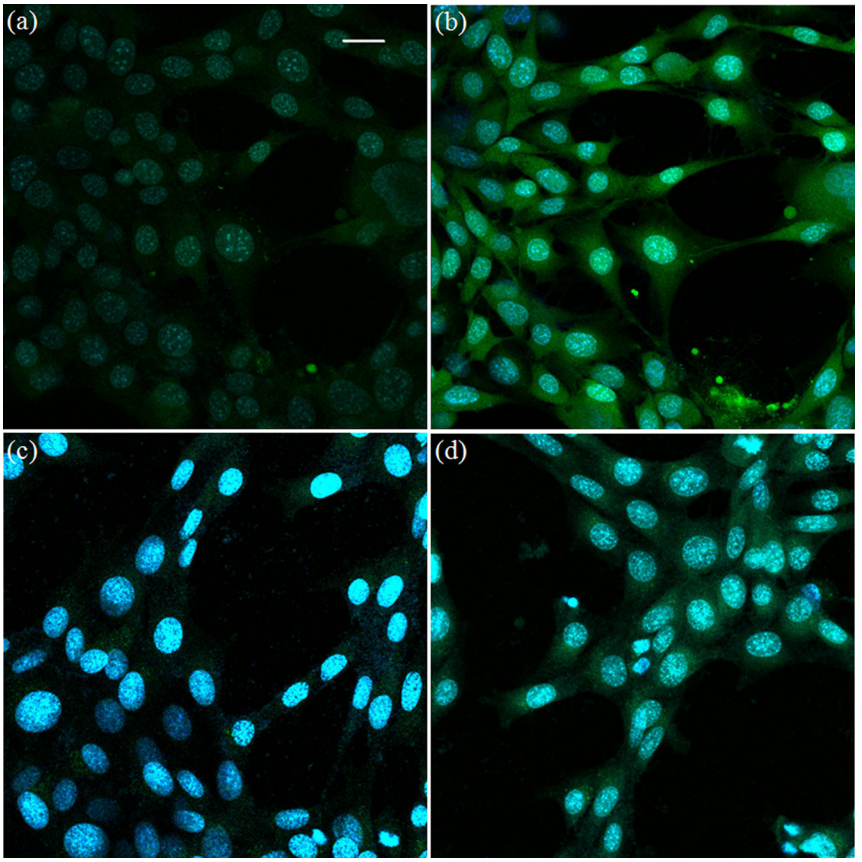

Fig. 3 Two-photon fluorescence (TPF) imaging of extra additional H_2O_2 and endogenous H_2O_2 in HT22 cells. TPF imaging in (a) 1 min and (b) 38 min after extra 50 μM H_2O_2 was added. TPF imaging in (c) 3 min and (d) 38 min after rotenone was added. The nuclei (blue), stained with Hoechst 33342, were co-excited with 770-nm wavelength laser pulses. Scale bar: 50 μm.

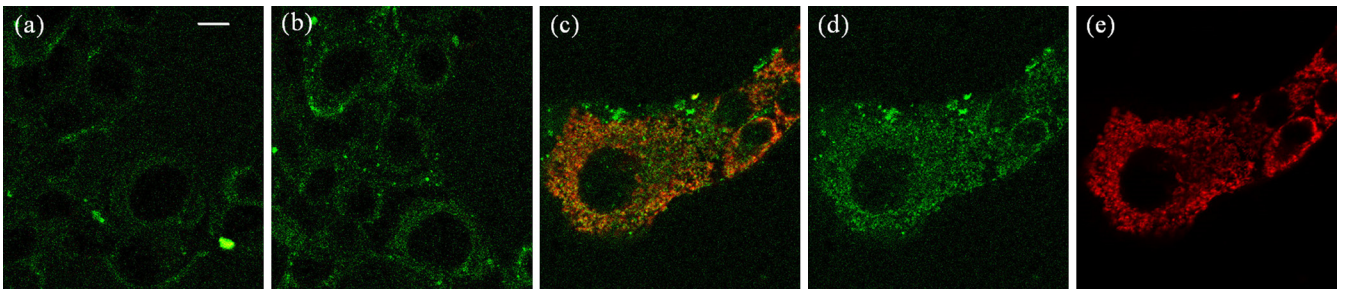

Fig. 4 TPF imaging of localized mitochondrial H_2O_2 in HT22 cells with MitoPY1. (a) TPF imaging of HT22 cells after MitoPY1 was incubated for 10 min. (b) TPF imaging of the cells after rotenone was added for 10 min. (c) TPF imaging shows the overlay of co-localization mitochondrial H_2O_2 production and cellular mitochondria after rotenone was added for 80 min. The green channel shows MitoPY1 signal (d) and the red channel shows MitoTracker Red signal (e). Both the MitoPY1 and MitoTracker Red dyes were co-excited with 770-nm wavelength laser pulses. Scale bar: 10 μm.

The real-time visualization of H_2O_2 production is another challenging issue that required a fast response of the fluorescent probes. Here, the chemoselective H_2O_2 probes showed much faster activation time compared with commercial probes such as DCF. It provides a more accurate technique for flow cytometric analysis of isolated cells or mitochondria and allows for the detection of changes such as cell activation, oxidative status, and cell death. Some probes have been successfully used to study ROS in a variety of biological systems with confocal microscopy.[31–34] Therefore, the combination of new fluorescent probes for H_2O_2 and the deep tissue imaging capability of two-photon microscopy may allow direct visualization of *in vivo* H_2O_2 dynamics in cells in their natural environment as well as their response to systematic manipulations.

4 Conclusions

This study introduces chemoselective probes for TPF imaging intracellular H_2O_2 production. TPA spectra were measured and TPF imaging was successfully demonstrated for cytoplasmic

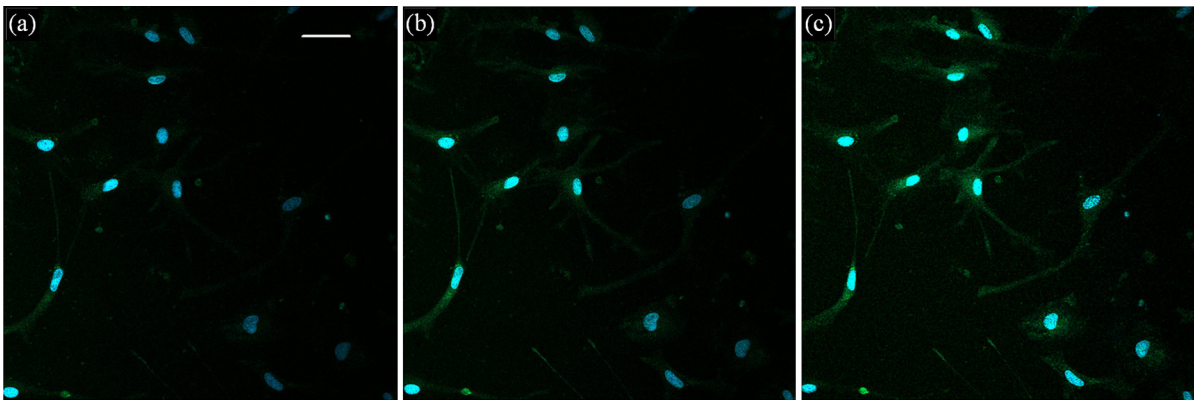

Fig. 5 TPF images of cytoplasmic H_2O_2 generation in astrocytes after (a) 1 min, (b) 6 min, and (c) 25 min after injection of D-alanine and FAD into the cells genetically modified with DAAO. The cells were loaded with 5 μM PF6-AM (green) for 30 min before use. The nuclei (blue), stained with Hoechst 33342, were co-excited with 770-nm wavelength laser pulses. Scale bar: 50 μm.

and mitochondrial H_2O_2 production in brain cells using PF6-AM and MitoPY1 probes. The probes showed high sensitivity and fast response to H_2O_2 detection. With the advantages of chemoselective probes, TFP imaging provides a novel opportunity for real-time monitoring of H_2O_2 detection and oxidative stress evaluation in live cells and *in vivo*.

Acknowledgments

This work is supported by the National Institutes of Health (NIH) Grant Nos. 2P01AG014930, 3R01 CA133148, R21AG042700, R21DK088066, R21EB012215, Dr. Miriam and Sheldon G. Adelson Medical Research Foundation. B.C.D. is a Fellow of the Jane Coffin Childs Memorial Fund for Medical Research. We acknowledge Christopher J. Chang, Demirhan Kobat, David Rivera, Anthony Fouad, Li Barie, Jian Zhong, and Jimmy B. Payappilly for technical support and helpful comments.

References

1. R. E. Haskew-Layton et al., "Controlled enzymatic production of astrocytic hydrogen peroxide protects neurons from oxidative stress via an Nrf2-independent pathway," *Proc. Natl. Acad. Sci. U.S.A.* **107**(40), 17385–17390 (2010).
2. B. C. Dickinson et al., "Nox2 redox signaling maintains essential cell populations in the brain," *Nat. Chem. Biol.* **7**(2), 106–112 (2011).
3. E. W. Miller et al., "Molecular imaging of hydrogen peroxide produced for cell signaling," *Nat. Chem. Biol.* **3**(5), 263–267 (2007).
4. S. G. Rhee, "H_2O_2, a necessary evil for cell signaling," *Science* **312**(5782), 1882–1883 (2006).
5. B. C. Dickinson and C. J. Chang, "Chemistry and biology of reactive oxygen species in signaling or stress responses," *Nat. Chem. Biol.* **7**(8), 504–511 (2011).
6. M. P. Murphy et al., "Unraveling the biological roles of reactive oxygen species," *Cell Metab.* **13**(4), 361–366 (2011).
7. P. Niethammer et al., "A tissue-scale gradient of hydrogen peroxide mediates rapid wound detection in zebrafish," *Nature* **459**(7249), 996–U123 (2009).
8. T. Finkel, M. Serrano, and M. A. Blasco, "The common biology of cancer and ageing," *Nature* **448**(7155), 767–774 (2007).
9. J. B. Pi et al., "Reactive oxygen species as a signal in glucose-stimulated insulin secretion," *Diabetes* **56**(7), 1783–1791 (2007).
10. K. J. Barnham, C. L. Masters, and A. I. Bush, "Neurodegenerative diseases and oxidative stress," *Nat. Rev. Drug Discov.* **3**(3), 205–214 (2004).
11. M. T. Lin and M. F. Beal, "Alzheimer's APP mangles mitochondria," *Nat. Med.* **12**(11), 1241–1243 (2006).
12. A. V. Rao and B. Balachandran, "Role of oxidative stress and antioxidants in neurodegenerative diseases," *Nutr. Neurosci.* **5**(5), 291–309 (2002).
13. C.-H. A. Chen, "Role of reactive oxygen species in low level light therapy," *Proc. SPIE* **7165**, 716502 (2009).
14. V. V. Belousov et al., "Genetically encoded fluorescent indicator for intracellular hydrogen peroxide," *Nat. Methods* **3**(4), 281–286 (2006).
15. B. Simen, Zhao et al., "A highly selective fluorescent probe for visualization of organic hydroperoxides in living cells," *J. Am. Chem. Soc.* **132**(48), 17065–17067 (2010)
16. J. P. Crow, "Dichlorodihydrofluorescein and dihydrorhodamine 123 are sensitive indicators of peroxynitrite in vitro: implications for intracellular measurement of reactive nitrogen and oxygen species," *Nitric Oxide* **1**(2), 145–157 (1997).
17. D. Lee et al., "In vivo imaging of hydrogen peroxide with chemiluminescent nanoparticles," *Nat. Mater.* **6**(10), 765–769 (2007).
18. B. C. Dickinson and C. J. Chang, "A targetable fluorescent probe for imaging hydrogen peroxide in the mitochondria of living cells," *J. Am. Chem. Soc.* **130**(30), 9638–9639 (2008).
19. L. N. Wu, X. J. Zhang, and H. X. Ju, "Highly sensitive flow injection detection of hydrogen peroxide with high throughput using a carbon nanofiber-modified electrode," *Analyst* **132**(5), 406–408 (2007).
20. A. R. Lippert, G. C. Van de Bittner, and C. J. Chang, "Boronate oxidation as a bioorthogonal reaction approach for studying the chemistry of hydrogen peroxide in living systems," *Acc. Chem. Res.* **44**(9), 793–804 (2011).
21. J. Chan, S. C. Dodani, and C. J. Chang, "Reaction-based small-molecule fluorescent probes for chemoselective bioimaging," *Nat. Chem.* **4**(12), 973–984 (2012).
22. B. C. Dickinson, C. Huynh, and C. J. Chang, "A palette of fluorescent probes with varying emission colors for imaging hydrogen peroxide signaling in living cells," *J. Am. Chem. Soc.* **132**(16), 5906–5915 (2010).
23. P. E. Hockberger et al., "Activation of flavin-containing oxidases underlies light-induced production of H_2O_2 in mammalian cells," *Proc. Natl. Acad. Sci. U. S. A.* **96**(11), 6255–6260 (1999).
24. J. M. Squirrell et al., "Long-term two-photon fluorescence imaging of mammalian embryos without compromising viability," *Nat. Biotechnol.* **17**(8), 763–767 (1999).
25. C. Chung et al., "A two-photon fluorescent probe for ratiometric imaging of hydrogen peroxide in live tissue," *Chem. Commun.* **47**(34), 9618–9620 (2011).
26. H. Guo et al., "Two-photon imaging of intracellular hydrogen peroxide with a chemoselective fluorescence probe," in *Optics in the Life Sciences*, OSA Technical Digest (CD), paper OTuD3, Optical Society of America, Monterey, California (2011).
27. Y. Chen et al., "Recent advances in two-photon imaging: technology developments and biomedical applications," *Chin. Opt. Lett.* **11**(1), 011703 (2013).
28. C. Xu and W. W. Webb, "Measurement of two-photon excitation cross sections of molecular fluorophores with data from 690 to 1050 nm," *J. Opt. Soc. Am. B* **13**(3), 481–491 (1996).

29. N. Y. Li et al., "Mitochondrial complex I inhibitor rotenone induces apoptosis through enhancing mitochondrial reactive oxygen species production," *J. Biol. Chem.* **278**(10), 8516–8525 (2003).
30. S. H. Huang, A. A. Heikal, and W. W. Webb, "Two-photon fluorescence spectroscopy and microscopy of NAD(P)H and flavoprotein," *Biophys. J.* **82**(5), 2811–2825 (2002).
31. J. Lu et al., "S100B and APP promote a gliocentric shift and impaired neurogenesis in down syndrome neural progenitors," *PLoS One* **6**(7), e22126 (2011).
32. Y. Ohsaki et al., "Increase of sodium delivery stimulates the mitochondrial respiratory chain H_2O_2 production in rat renal medullary thick ascending limb," *Am. J. Physiol-Renal* **302**(1), F95–F102 (2012).
33. J. F. Woolley et al., "H_2O_2 production downstream of FLT3 is mediated by p22phox in the endoplasmic reticulum and is required for STAT5 signalling," *PLoS One* **7**(7), e34050 (2012).
34. J. Sakai et al., "Reactive oxygen species-induced actin glutathionylation controls actin dynamics in neutrophils," *Immunity* **37**(6), 1037–1049 (2012).